Mon. Not. R. Astron. Soc. **000**, 000–000 (0000) Printed 24 February 2013 (MN LATEX style file v2.2)

Gravitational Wave Heating of Stars and Accretion Disks

Gongjie Li, Bence Kocsis, Abraham Loeb
Institute for Theory & Computation, Harvard-Smithsonian Center for Astrophysics, Cambridge, MA, USA

arXiv:1203.0317v2 [astro-ph.HE] 27 Apr 2012

24 February 2013

ABSTRACT
We investigate the electromagnetic (EM) counterpart of gravitational waves (GWs) emitted by a supermassive black hole binary (SMBHB) through the viscous dissipation of the GW energy in an accretion disk and stars surrounding the SMBHB. We account for the suppression of the heating rate if the forcing period is shorter than the turnover time of the largest turbulent eddies. We find that the viscous heating luminosity in $0.1M_\odot$ stars can be significantly higher than their intrinsic luminosity, but still too low to be detected for extragalactic sources. The relative brightening is small for accretion disks.

Key words: black hole physics – galaxies: nuclei – gravitational waves

1 INTRODUCTION

The coalescence of supermassive black hole binaries (SMBHBs) generates gravitational waves (GW) which are a primary source for the proposed Laser Interferometric Space Antenna (LISA[1]). SMBHBs are inevitable outcomes of galaxy mergers. Spatially-resolved active galactic nuclei have been observed (Komossa et al. 2003; Bianchi et al. 2008; Green et al. 2010; Koss et al. 2011; Fabbiano et al. 2011). In addition, spectroscopic surveys (Comerford et al. 2009; Smith et al. 2010; Liu et al. 2010b) and observations that combine ground-based imaging show numerous systems containing compelling SMBHB candidates with pc to kpc separations (Rodriguez et al. 2006; Liu et al. 2010a; Shen et al. 2011; Fu et al. 2011; McGurk et al. 2011). Hydrodynamic simulations of galaxy mergers also predict SMBHB pair formation (e.g. Escala et al. 2004, 2005; Di Matteo et al. 2005; Robertson et al. 2006; Hopkins et al. 2006; Callegari et al. 2009; Colpi et al. 2009; Blecha et al. 2012).

Electromagnetic (EM) counterparts to GW sources complements the GW detection by determining the host galaxy redshift and the environment of the sources (Kocsis et al. 2006; Phinney 2009). A large variety of EM signatures have been proposed to accompany the coalescence of SMBHBs (Schnittman 2011; Haiman et al. 2009). In the pre-merger phase, the torques of the SMBHB excavates a hollow region in the disk and leads to periodic accretion across the gap on the orbital timescale (Cuadra et al. 2009; MacFadyen & Milosavljević 2008; Hayasaki et al. 2008). After the merger, the recoil of the black hole remnant and its sudden mass loss due to the final GW burst produce shocks in the accretion disk which lead to EM signals (Bode & Phinney 2007; Lippai et al. 2008; Schnittman & Krolik 2008; Shields & Bonning 2008; O'Neill et al. 2009; Rossi et al. 2010). The recoil of the black hole remnant changes the tidal disruption rate of stars due to the refilling of the loss cone and the wandering of black hole remnant (Stone & Loeb 2011a,b; Li et al. 2012). Finally, the infall of gas onto the black hole remnant produces an EM afterglow (Milosavljević & Phinney 2005; Tanaka & Menou 2010).

In this paper, we consider the viscous dissipation of GWs generated by a SMBHB in a neighboring gaseous medium. In particular, the velocity shear induced by GWs in the gas is damped by viscosity. The dissipated GW energy turns into heat, and produces an electromagnetic flare. Unlike other EM counterparts, the brightening here follows promptly within a few hours to days after the coalescence of the SMBHB (Kocsis & Loeb 2008). The effect provides a unique test of general relativity for the interaction of GWs with matter. In § 2 and 3 we investigate GW dissipation in a gaseous accretion disk and stars in the vicinity of the SMBHB. We examine the suppression of the effect if the forcing period is shorter than the turnover time of the largest eddies (Krolik 2010), in analogy to a similar treatment of tidal heating in binary stars (Zahn 1966; Goldreich & Keeley 1977). Finally, we discuss our conclusions and their implications in § 4.

2 METHOD

We start by presenting our approach for estimating the GW heating inside an accretion disk and stars due to turbulent viscosity. Following Kocsis & Loeb (2008), we approximate the GW luminosity by matching the Newtonian inspiral luminosity prior to merger ($t < 0$), the peak luminosity at the merger ($t = 0$) and the decay luminosity afterwards ($t > t_1$),

[1] http://lisa.nasa.gov/

© 0000 RAS

where t_1 can be fixed from this matching procedure. Specifically, in the Newtonian inspiral regime, the luminosity is

$$L_{\rm GW\,inspiral} = \frac{32}{5}\frac{G^4}{c^5}\frac{M^3\mu^2}{a^5}, \quad (1)$$

where $M = M_1+M_2$ is the sum of the masses of the SMBHB members, $\mu = M_1M_2/M$ is the reduced mass of the SMBHB and a is the separation between the SMBHB, which can be expressed as

$$a = \left[\frac{256}{5}\frac{G^3}{c^5}\mu M^2(t_1-t)\right]^{1/4}, \quad (2)$$

assuming a circular orbit. The peak luminosity is approximated from numerical simulations (Berti et al. 2007; Buonanno et al. 2007) as

$$L_{\rm GW\,peak} \approx 10^{-3}\frac{c^5}{G}\Big(\frac{\mu}{M}\Big)^2, \quad (3)$$

and the ringdown luminosity is set to be

$$L_{\rm GW\,ringdown} = L_{\rm GW\,peak}\exp\Big(-\frac{c(t-t_1)}{5R_{\rm g}}\Big), \quad (4)$$

where $R_{\rm g} = GM/c^2$ is the gravitational radius of the SMBHB. The peak luminosity is modified by a factor of two (Berti et al. 2007; Buonanno et al. 2007) due to different magnitudes and orientation of the spin of the SMBHB. In this paper, we assume the masses of the two black holes are the same.

With the approximated expression of GW luminosity as a function of time, the dissipation of GW energy inside a viscous medium can be calculated by solving the weak-field Einstein equation (Hawking 1966; Weinberg 1972):

$$\dot{e}_{\rm heat} = \frac{16\pi G\eta}{c^2}e_{\rm GW}, \quad (5)$$

where $\dot{e}_{\rm heat}$ is the dissipation rate, η is the dynamical viscosity and $e_{\rm GW}$ is the GW energy density. $e_{\rm GW}$ can be obtained from $e_{\rm GW} = Y(\theta)\frac{L_{\rm GW}}{4\pi cr^2}$, where θ is the angle relative to the total angular momentum vector, $Y(\theta) = 5/2[\sin^8(\theta/2)+\cos^8(\theta/2)]$. We use the average value $\langle Y\rangle = 1$ below. With $L_{\rm GW}$ derived, the only unknown parameter is the dynamical viscosity of the medium that the GW passes through. The dissipation rate of the GW energy gives the heating rate of any gaseous medium such as an accretion disk and stars.

Next, we estimate the dynamical viscosity for stars. We use stellar models produced by Modules for Experiments in Stellar Astrophysics (MESA[2]) (Paxton et al. 2011), a 1D stellar evolution code, and we consider stellar models, whose properties are included in Table 1. We associate the dynamical viscosity with the mixing length theory diffusion coefficient, which is directly provided in the simulated models by MESA. When the period of the driving force is smaller than the largest eddy turnover time, the eddy viscosity depends on the ratio of the period to the largest eddy turnover time in one of two possible ways:

$$\eta = \eta_i\ \min\Big[\Big(\frac{\tau_{\rm GW}}{2\tau_l}\Big), 1\Big], \quad (6)$$

[2] http://mesa.sourceforge.net/

or

$$\eta = \eta_i\ \min\Big[\Big(\frac{\tau_{\rm GW}}{2\pi\tau_l}\Big)^2, 1\Big], \quad (7)$$

where η_i is the intrinsic viscosity in the absence of shear force with short period, τ_l is the largest eddy turnover timescale and $\tau_{\rm GW}$ is the shear force period, which is calculated as $2\pi/\omega_{\rm GW}$, where $\omega_{\rm GW} = 2\sqrt{GM/a^3}$ in the inspiral phase $a < 6R_{\rm g}$ and $0.25/(GM/c^3)$] after the ringdown, and extrapolate linearly during the transition according to Buonanno et al. (2007). The viscosity scaling given by Eq. (6) is discussed in Zahn (1966, 1989); Zahn & Bouchet (1989) and Eq. (7) in Goldreich & Keeley (1977); Goldreich & Nicholson (1989). Observations are more consistent with Zahn's scaling for pulsating stars in the red edge of the instability strip (Gonczi 1982), for tidal circularization of binary stars (Verbunt & Phinney 1995; Meibom & Mathieu 2005), while the damping of the solar p-mode oscillations is more consistent with the Goldreich's scaling (Goldreich & Kumar 1988; Goldreich et al. 1994). Recently, Penev et al. (2009) studied turbulent viscosity in low mass stars using the perturbative approach of Goodman & Oh (1997), taking into account compressible fluid and anisotropic viscosity. Their simulation suggests a linear scaling. However, Ogilvie & Lesur (2012) found results more consistent with Goldreich's scaling when studying the limit of a low amplitude short oscillation period shear. We considered both scalings for stars in this paper.

With the viscosity for stars and $L_{\rm GW}(t)$ in hand, the GW heating rate can be estimated using Eq. (5). The EM luminosity increase can be estimated by solving the radiative transfer equation:

$$t_c(r)\frac{d}{dt}\Delta f(r) + \Delta f(r) = \dot{e}_{\rm heat}, \quad (8)$$

$$L_{\rm GWH} = \int_{\rm star}\Delta f(r)\ dV, \quad (9)$$

where $\Delta f(r)$ is the excess EM signal produced per unit volume as a function of location in the star, $L_{\rm GWH}$ is the excess EM luminosity associated to GW heating, and $t_c(r)$ is the cooling time as a function of the location, which characterizes the time it takes for heat to travel to the surface. We estimate the latter by taking the integral of the minimum of the photon diffusion time, $dr/c\times[\tau(r)-(R_*-r)\frac{d\tau(r)}{dr}]$, and the turbulent convection time, $dr/v_c(r)$, in each spherical shell inside the star, where the optical depth, $\tau(r)$, and the convective velocity, $v_c(r)$ are obtained from the MESA simulation, and R_* is the radius of the star.

Finally, we estimate the heating in accretion disks. We adopt the geometrically thin, optically thick, standard accretion disk model, where the angular momentum transport is associated with the internal stresses due to turbulence (Shakura & Sunyaev 1973; Novikov & Thorne 1973). Heat is dissipated locally by turbulent viscosity, and transported vertically outward by photon diffusion or advection. Specifically, the viscosity of the accretion disk is

$$\eta_i(r) = \frac{2}{3}\frac{\alpha P(r)}{\Omega(r)}, \quad (10)$$

where $\Omega^2(r) = GM/r^3$ is the angular velocity, α is a constant which we assume to be 0.3 (King et al. 2007), and P is the total (gas+radiation) pressure in the α disk model, and gas pressure in the β model. In these models, the physical

characteristics of the disk is fixed by the following parameters: the accretion rate in Eddington units ($\dot{m}$), the radiation efficiency (ϵ), and the SMBHB mass (M) (Goodman 2003; Goodman & Tan 2004). We set $\dot{m}$ to be 0.1, ϵ to be 0.1, and discuss the effects caused by different SMBHB masses.

Similarly to stars, we account for the frequency dependence of viscosity when the period of the driving force is smaller than the largest eddy turnover time, and estimate the effective viscosity according to the perturbative methods as discussed in Goodman & Oh (1997). Specifically, for incompressible fluid with isotropic viscosity, the viscosity as a function of driving force frequency can be expressed in terms of the frequency spectrum of the average kinetic energy per unit mass. For accretion disks, where the Kolmogorov scalings may not be applicable to obtain the energy spectrum, we adopt the energy spectrum from recent magnetohydrodynamic (MHD) disk simulations. Flock et al. (2011) present a full 2π three dimensional simulation on a stratified accretion disk, where the turbulence is driven by magnetorotational instability (MRI) and the kinetic spectra is obtained in the ϕ direction, and Fromang (2010) investigate the MRI in a shearing box with zero net flux. Flock et al. (2011) and Fromang (2010) estimate the kinetic energy spectrum exponent to be 11/9 and 1.5, respectively. We estimate the viscous heating in accretion disk with the Flock et al. (2011) exponent as well as the Kolmogorov scaling exponent 2.

Similarly to the calculation for stars, the GW heating rate can be estimated using Eq. (5). The corresponding EM signals can be estimated by solving the radiative transfer equation following Kocsis & Loeb (2008):

$$t_c(r)\frac{d}{dt}\Delta F(r,t) + \Delta F(r,t) = H\dot{e}_{\rm heat}(r,t), \quad (11)$$

$$L_{\rm GWH}(t) = \int_{r_{\rm min}}^{r_{\rm max}} 2\pi r \Delta F(r,t)\, dr, \quad (12)$$

where $F(r)$ is the excess EM flux due to GW heating in the accretion disk, H is the scaleheight, $L_{\rm GWH}$ is the corresponding excess EM luminosity, and $t_c(r)$ is the cooling time. Here, we assume the disk is face on, and account for the different light-travel time from different annuli in the disk. The brightening can be somewhat larger in an inclined or edge-on configuration (by up to a factor of ~ 3) where the peak GW flux is observed coincidentally at the inner and outer radii along the line of sight (Kocsis & Loeb 2008).

3 RESULTS

First, we consider the GW heating of nearby stars. As an example, we examine the GW heating light curve for a 0.1 $M_\odot$ star (stellar model 2) surrounding an $M = 10^7$ or an $10^9 M_\odot$ SMBHB, respectively. Using Eqs. (8) and (9), we calculate $F(t)$ and plot the GW heating light curve in Figure 1. We assume that the star is located at $d = 5$ tidal radii from the SMBHB (corresponds to 320 and 15 $R_{\rm g}$ for a 10^7 and a 10^9 $M_\odot$ SMBHB, respectively). Note that since the GW luminosity is proportional to $(d/R_{\rm g})^{-2}$, the GW heating effect is much larger around more massive SMBHBs because the viscosity suppression for a high mass SMBHB is smaller.

Figure 1 shows that the excess luminosity of the star surrounding the $10^9 M_\odot$ SMBHB is much higher than the intrinsic luminosity of the star ($L = 2.6\times10^{30}$erg s^{-1}). In fact,

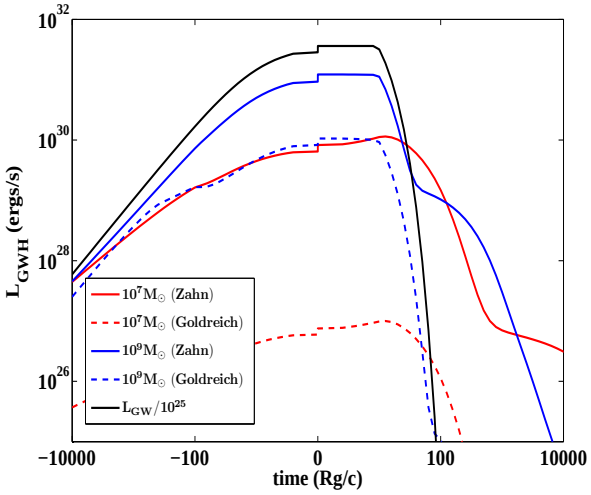

Figure 1. The light curve of a GW heated star (based on star model 2 with an intrinsic luminosity: $L = 2.6\times10^{30}$erg s^{-1}). The time axis is in units of $R_{\rm g}/c$, and is shown on a logarithmic scale at both negative and positive values (causing the discontinuity at $t = 0$). The star is located 5 tidal radii away from the SMBHB (320 and 15 $R_{\rm g}$ for a 10^7 $M_\odot$ and 10^9 $M_\odot$ SMBHB, respectively). The black line indicates the GW luminosity scaled down by 25 order of magnitude in order to fit in this figure. The red and blue lines indicate the light curve of a star surrounding a 10^7 and a 10^9 $M_\odot$ SMBHB, respectively, with solid and dashed lines corresponding to the viscosity dependence with $(\tau_{\rm GW}/2\tau_l)$ and $(\tau_{\rm GW}/2\pi\tau_l)^2$, respectively. The light curve closely tracks the GW light curve. Interestingly, the peak luminosity surrounding the 10^9 $M_\odot$ SMBHB is much higher than the intrinsic luminosity of this star.

the net dissipated GW energy can exceed the gravitational binding energy near the stellar surface, and could generate a stellar wind. However, as the viscosity is strongly suppressed in the stellar interior ($\frac{\tau_{\rm GW}}{\tau_l(r)} \ll 1$ for $r \lesssim 0.99 R_{star}$), the heating effect is negligible to the star as a whole. In addition, these stars are very faint; the absolute peak GW heating luminosity in the star is typically too faint to be observed outside of the Galaxy.

Since the turnover time of turbulent eddies is much longer in the interior of the star than that at the surface, the energy is mostly dissipated at the surface. Since the cooling time near the surface (~ 200 s) is short compared to the peak GW timescale ($\sim 10\, R_g/c \sim 500\,{\rm s}\, M_{\rm BH}/10^7\, M_\odot$), the light curve of the star closely tracks the luminosity curve of the GW. When the GW driving period is shorter than the eddy turnover time, the viscosity caused by the eddy depends on the ratio $\tau_{\rm GW}/\tau_l$, where the exact scaling is uncertain as discussed in § 2. For stars surrounding a 10^9 $M_\odot$ SMBHB, the differences between the two scalings are smaller as the period of peak GW emission for this SMBHB mass is more comparable to the surface eddy turnover time in a 0.1 $M_\odot$ star.

To examine the influence of the GW heating in different types of stars, we consider stellar models of different stellar masses and ages as included in Table 1. We include the extreme cases with 0.1 $M_\odot$ and 100 $M_\odot$ stars. We plot the ratio of the peak heating luminosity to the intrinsic luminosity for different stellar models in Figure 2 with Zahn's scaling. We

Table 1. Properties of stellar models

No.	Mass ($M_\odot$)	Metallicity (Z)	Radius ($R_\odot$)	Luminosity ($L_\odot$)	Age (yrs)
1	0.1	0.16	3.3	0.00079	2×10^4
2	0.1	0.16	3	0.00066	5×10^6
3	0.1	0.16	0.57	5.5×10^{-5}	2×10^9
4	0.1	0.01	2.4	0.43	2×10^4
5	0.1	0.01	0.44	0.022	5×10^6
6	0.1	0.01	0.12	0.0012	2×10^9
7	100	0.04	21	1.4×10^6	1×10^4
8	100	0.04	36	1.7×10^6	1×10^6
9	100	0.04	960	2.1×10^6	2×10^6

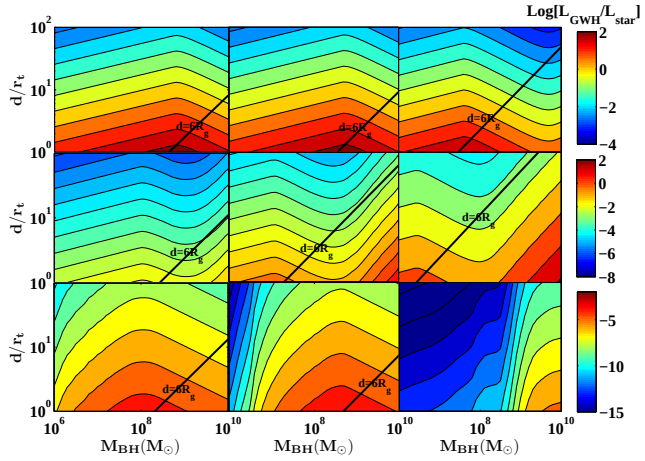

Figure 2. Ratio of the peak GW heating luminosity to the intrinsic stellar luminosity. The horizontal axis shows the mass of the SMBHB, and the vertical axis plots the distance (d) between the star and the SMBHB in units of the tidal radius (r_t). First row: model 1, 2, 3; second row: model 4, 5, 6, third row: model 7, 8, 9. Solid black line indicates where the distance between the star and black hole binary is 6 $R_{\rm g}$, the radius of the innermost stable circular orbit (ISCO) around a non-spinning black hole. In the last panel, the points in the figure lie out of 6 $R_{\rm g}$, and so the black line is not shown. The first two rows correspond to 0.1 $M_\odot$ stars with metallicity $Z=0.16$ and $Z=0.01$ respectively, and the last row corresponds to 100 $M_\odot$ stars. GW heating is most significant for high metallicity low mass stars.

find that the influence of the GW heating is more significant as the metallicity of the star increases, and GW heating is not significant for very massive ($M_*\geq100M_\odot$) stars.

Next, we discuss the heating effects in accretion disks. For α and β disks, we solve Eqs. (11) and (12) for the heating flux, and plot the heating light curve of the disk due to GW heating in Figure 3. The accretion disk is punctured with an inner hole. This geometry is essentially "frozen" during the final GW merger timescale with a gap radius $\gtrsim 100M$ for α–disks (Milosavljević & Phinney 2005). Recent MHD simulations by Noble et al. (2012) indicate that the stresses may be enhanced in a binary, such that gap decoupling occurs further in, at $20R_{\rm g}$. We optimistically adopt this value for our estimates, which implies a larger heating rate than that for a larger gap radius. We integrate over the

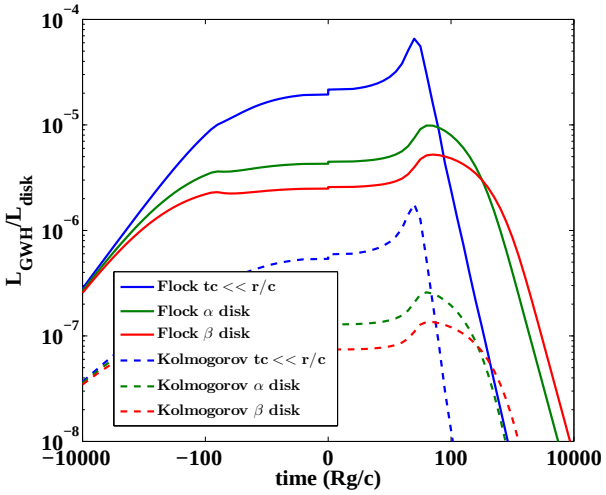

Figure 3. The excess luminosity relative to the disk luminosity due to GW heating on an accretion disk (inner disk truncated at 20 $R_{\rm g}$) before ($t<0$) and after ($t>0$) the binary coalescence event. The time axis is shown on a logarithmic scale at both negative and positive values (in units of $R_{\rm g}$). The SMBHB mass is $10^7M_\odot$. Solid lines corresponds to the frequency dependence $(\tau_{\rm GW}/2\pi\tau_l)^{\frac{11}{9}}$ derived according to the energy spectrum of accretion disk based on MHD simulations by Flock et al. (2011), and the dashed lines correspond to the scaling $(\tau_{\rm GW}/2\pi\tau_l)^2$, assuming Kolmogorov turbulence.

accretion disks between the inner and outer boundary. We set the latter to $2\times10^4R_{\rm g}$, but this value does not influence our result as the heating in the outer accretion disk is negligible. We include the different light travel time from different accretion disk surface elements along the line of sight. Our calculation of the heating in the accretion disks improves the simplified treatment of Kocsis & Loeb (2008) by including the dependence of viscosity on the ratio of the GW driving period to the largest eddy turnover time, which suppresses the dissipation of GWs. We consider two cases in this plot. Following the perturbative turbulence derivation by Goodman & Oh (1997), the power-law index is 2 for Kolmogorov turbulent scaling, and $\frac{11}{9}$ according to MHD disk simulation by Flock et al. (2011). The eddy turnover time increases rapidly as the radius increases, and so the suppression of the GW heating is less significant for disks truncated closer to the SMBHB. Therefore, the heating luminosity is more significant for disks that are truncated closer to the SMBHB.

4 DISCUSSION

In this paper, we considered the dissipation of GWs in an accretion disk or stars surrounding a SMBHB. We have found that the GW heating luminosity of the accretion disk and stars are low, and make no significant EM flare relative to their intrinsic luminosity except for low mass stars ($\sim0.1M_\odot$). The integrated excess luminosity from heated low mass stars is too low to be observed in galactic nuclei as they are faint. Assuming a Bahcall-Wolf distribution of stars or assuming a collision timescale larger than 1 Myr, we find that only a few stars are expected to be within 5 tidal

radii of a coalescing SMBHB, where the GW heating effect is significant. Therefore the overall brightening of the stellar cluster is negligible.

In order to be heated significantly by GWs, the stars need to be close to the SMBHB. One possible avenue is that stars get caught in mean motion resonances (such as Trojan resonances) and move inwards as the SMBHB merge (Seto & Muto 2010; Schnittman 2010). This is only effective for SMBHB with an unequal mass ratio $q \lesssim 10^{-2}$; the stars get ejected before the coalescence otherwise. Another possibility is for stars to get captured or form in the outer parts of accretion disks, and migrate inwards by processes analogous to planetary migration (Miralda-Escudé & Kollmeier 2005; Karas & Šubr 2001; Levin 2007).

We assumed that GW energy is dissipated locally through turbulent viscosity. The damping of shear stress by eddy viscosity in stars was found to be consistent with observations in the context of the tidal circularization of binaries (Verbunt & Phinney 1995; Meibom & Mathieu 2005). The underlying accretion disk model is uncertain since the disk structure is unstable to both thermal and viscous instabilities. Recently, Blaes et al. (2011) found that radiation-dominated disks differ significantly from the standard disk models, where the dissipation associated with the turbulent cascade and radiative damping dissipate energy non-locally. It remains to be seen whether the GW heating effect is more prominent in alternative disk models.

ACKNOWLEDGMENTS

We thank Eliot Quataert, Sterl Phinney and Paul Groot for helpful discussions. This work was supported in part by NSF grant AST-0907890 and NASA grants NNX08AL43G and NNA09DB30A. BK acknowledges support from NASA through Einstein Postdoctoral Fellowship Award Number PF9-00063 issued by the Chandra X-ray Observatory Center, which is operated by the Smithsonian Astrophysical Observatory for and on behalf of the National Aeronautics Space Administration under contract NAS8-03060.

REFERENCES

Berti E., Cardoso V., Gonzalez J. A., Sperhake U., Hannam M., Husa S., Brügmann B., 2007, PRD, 76, 064034
Bianchi S., Chiaberge M., Piconcelli E., Guainazzi M., Matt G., 2008, MNRAS, 386, 105
Blaes O., Krolik J. H., Hirose S., Shabaltas N., 2011, ApJ, 733, 110
Blecha L., Loeb A., Narayan R., 2012, ArXiv e-prints
Bode N., Phinney S., 2007, APS April Meeting Abstracts, 1010
Buonanno A., Cook G. B., Pretorius F., 2007, PRD, 75, 124018
Callegari S., Mayer L., Kazantzidis S., Colpi M., Governato F., Quinn T., Wadsley J., 2009, ApJL, 696, L89
Colpi M., Callegari S., Dotti M., Mayer L., 2009, Classical and Quantum Gravity, 26, 094029
Comerford J. M., Gerke B. F., Newman J. A., Davis M., Yan R., Cooper M. C., Faber S. M., Koo D. C., Coil A. L., Rosario D. J., Dutton A. A., 2009, ApJ, 698, 956
Cuadra J., Armitage P. J., Alexander R. D., Begelman M. C., 2009, MNRAS, 393, 1423
Di Matteo T., Springel V., Hernquist L., 2005, Nature, 433, 604
Escala A., Larson R. B., Coppi P. S., Mardones D., 2004, ApJ, 607, 765
—, 2005, ApJ, 630, 152
Fabbiano G., Wang J., Elvis M., Risaliti G., 2011, Nature, 477, 431
Flock M., Dzyurkevich N., Klahr H., Turner N. J., Henning T., 2011, ApJ, 735, 122
Fromang S., 2010, AAP, 514, L5
Fu H., Zhang Z.-Y., Assef R. J., Stockton A., Myers A. D., Yan L., Djorgovski S. G., Wrobel J. M., Riechers D. A., 2011, ApJL, 740, L44
Goldreich P., Keeley D. A., 1977, ApJ, 212, 243
Goldreich P., Kumar P., 1988, ApJ, 326, 462
Goldreich P., Murray N., Kumar P., 1994, ApJ, 424, 466
Goldreich P., Nicholson P. D., 1989, ApJ, 342, 1079
Gonczi G., 1982, AAP, 110, 1
Goodman J., 2003, MNRAS, 339, 937
Goodman J., Oh S. P., 1997, ApJ, 486, 403
Goodman J., Tan J. C., 2004, ApJ, 608, 108
Green P. J., Myers A. D., Barkhouse W. A., Mulchaey J. S., Bennert V. N., Cox T. J., Aldcroft T. L., 2010, ApJ, 710, 1578
Haiman Z., Kocsis B., Menou K., Lippai Z., Frei Z., 2009, Classical and Quantum Gravity, 26, 094032
Hawking S. W., 1966, ApJ, 145, 544
Hayasaki K., Mineshige S., Ho L. C., 2008, ApJ, 682, 1134
Hopkins P. F., Somerville R. S., Hernquist L., Cox T. J., Robertson B., Li Y., 2006, ApJ, 652, 864
Karas V., Šubr L., 2001, AAP, 376, 686
King A. R., Pringle J. E., Livio M., 2007, MNRAS, 376, 1740
Kocsis B., Frei Z., Haiman Z., Menou K., 2006, ApJ, 637, 27
Kocsis B., Loeb A., 2008, Physical Review Letters, 101, 041101
Komossa S., Burwitz V., Hasinger G., Predehl P., Kaastra J. S., Ikebe Y., 2003, ApJL, 582, L15
Koss M., Mushotzky R., Treister E., Veilleux S., Vasudevan R., Miller N., Sanders D. B., Schawinski K., Trippe M., 2011, ApJL, 735, L42
Krolik J. H., 2010, ApJ, 709, 774
Levin Y., 2007, MNRAS, 374, 515
Li S., Liu F. K., Berczik P., Chen X., Spurzem R., 2012, ArXiv e-prints
Lippai Z., Frei Z., Haiman Z., 2008, ApJL, 676, L5
Liu X., Greene J. E., Shen Y., Strauss M. A., 2010a, ApJL, 715, L30
Liu X., Shen Y., Strauss M. A., Greene J. E., 2010b, ApJ, 708, 427
MacFadyen A. I., Milosavljević M., 2008, ApJ, 672, 83
McGurk R. C., Max C. E., Rosario D. J., Shields G. A., Smith K. L., Wright S. A., 2011, ApJL, 738, L2
Meibom S., Mathieu R. D., 2005, ApJ, 620, 970
Milosavljević M., Phinney E. S., 2005, ApJL, 622, L93
Miralda-Escudé J., Kollmeier J. A., 2005, ApJ, 619, 30
Noble S. C., Mundim B. C., Nakano H., Krolik J. H., Campanelli M., Zlochower Y., Yunes N., 2012, ArXiv e-prints
Novikov I. D., Thorne K. S., 1973, in Black Holes (Les

Astres Occlus), C. Dewitt & B. S. Dewitt, ed., pp. 343–450
Ogilvie G. I., Lesur G., 2012, ArXiv e-prints
O'Neill S. M., Miller M. C., Bogdanović T., Reynolds C. S., Schnittman J. D., 2009, ApJ, 700, 859
Paxton B., Bildsten L., Dotter A., Herwig F., Lesaffre P., Timmes F., 2011, ApJS, 192, 3
Penev K., Sasselov D., Robinson F., Demarque P., 2009, ApJ, 704, 930
Phinney E. S., 2009, in ArXiv Astrophysics e-prints, Vol. 2010, astro2010: The Astronomy and Astrophysics Decadal Survey, p. 235
Robertson B., Bullock J. S., Cox T. J., Di Matteo T., Hernquist L., Springel V., Yoshida N., 2006, ApJ, 645, 986
Rodriguez C., Taylor G. B., Zavala R. T., Peck A. B., Pollack L. K., Romani R. W., 2006, ApJ, 646, 49
Rossi E. M., Lodato G., Armitage P. J., Pringle J. E., King A. R., 2010, MNRAS, 401, 2021
Schnittman J. D., 2010, ApJ, 724, 39
—, 2011, Classical and Quantum Gravity, 28, 094021
Schnittman J. D., Krolik J. H., 2008, ApJ, 684, 835
Seto N., Muto T., 2010, PRD, 81, 103004
Shakura N. I., Sunyaev R. A., 1973, AAP, 24, 337
Shen Y., Liu X., Greene J. E., Strauss M. A., 2011, ApJ, 735, 48
Shields G. A., Bonning E. W., 2008, ApJ, 682, 758
Smith K. L., Shields G. A., Bonning E. W., McMullen C. C., Rosario D. J., Salviander S., 2010, ApJ, 716, 866
Stone N., Loeb A., 2011a, MNRAS, 412, 75
—, 2011b, ArXiv e-prints
Tanaka T., Menou K., 2010, ApJ, 714, 404
Verbunt F., Phinney E. S., 1995, AAP, 296, 709
Weinberg S., 1972, Gravitation and Cosmology: Principles and Applications of the General Theory of Relativity, Weinberg, S., ed.
Zahn J. P., 1966, Annales d'Astrophysique, 29, 489
Zahn J.-P., 1989, AAP, 220, 112
Zahn J.-P., Bouchet L., 1989, AAP, 223, 112